STUDY ON THE SYNCHROTRON DYNAMICS IN THE COMPTON X-RAY RING

E.V. Bulyak, P.I. Gladkikh, V.V. Skomorokhov
National Science Center "Kharkov Institute of Physics and Technology", Kharkov, Ukraine
e-mail: bulyak@kipt.kharkov.ua

The longitudinal dynamics of electron bunches with a large energy spread circulating in the storage rings with a small momentum compaction factor is considered. Also the structure of the longitudinal phase space is considered as well as its modification due to changes in the ring parameters. The response of an equilibrium area upon changes of the nonlinear momentum compaction factor is presented.

PACS: 41.60.-m, 52.59.-f, 52.38-r

1. INTRODUCTION

Engagement of electron storage rings for production of x rays through Compton scattering of laser photons against ultra-relativistic electrons was proposed in 1998 [1]. Two basic schemes exist so far. One of them supposes use of electron beams with unsteady parameters [2] and applies the continual injection (and ejection of circulating bunches by the next injecting pulse) of dense intensive bunches. The second scheme is based on the continuous circulation of bunches. To confine the bunches acquired a sufficiently large energy spread (see [3]), a lattice with a small controllable momentum compaction factor is proposed to employ [4]. Longitudinal dynamics in the small compaction factor lattice is governed not only by the linear effects of the momentum deviation but by the nonlinear ones as well.

In Compton sources storing the bunches with the large energy spread which can be as high as a few percents, ring's energy acceptance becomes compared to the energy spread. To get proper lifetime of the circulating electrons, the energy acceptance $\sigma \equiv \max (E\text{-}E_s)/E_s$ (E_s is the energy of synchronous particle) should be high enough.

Within a linear approximation according to the energy deviation, the acceptance can be increased either by enhancement of the radio frequency (rf) voltage, V_{rf}, or by decreasing of the linear momentum compaction factor α_0 since $\sigma \propto (V_{rf} / \alpha_0)^{1/2}$.

The paper presents result of study on the longitudinal dynamics of electron bunches circulating in storage rings with a small linear momentum compaction factor α_0. Structure of the phase space is considered and its deformation with changes in the ring lattice parameters. In particular, the size of stable area as a function of the rf voltage and momentum compaction is evaluated.

2. FINITE-DIFFERENCE MODEL

Let us consider a model of the ring comprised only two components: a drift and an rf cavity. For the sake of simplicity we will suggest the cavity infinitely short, in which the particle momentum (energy) suffer an abrupt change while the phase of a particle remains unchanged. On the contrary, the phase of a particle traveling along the drift changes while the energy remains invariable. The longitudinal motion in such idealized ring will be described in canonically conjugated variables ϕ (the phase about zero voltage in the cavity) and the momentum $p \equiv (\gamma - \gamma_s)/\gamma_s$ equal to the relative deviation of the particle energy from the synchronous one (γ_s is the Lorentz factor of the synchronous particle).

To study systems able to confine the beams with large energy spread, one needs to account not only the linear part of the orbit deviation from the synchronous one, but nonlinear terms as well:

$$\Delta x \approx D_1 p + D_2 p^2 + \dots , \tag{1}$$

where D_1 and D_2 are the dispersion functions of the first and second orders, respectively.

Accordingly, relative lengthening of a (flat) orbit is

$$\frac{\Delta L}{L_0} = \oint \sqrt{\left(1 + \frac{\Delta x}{\rho}\right)^2 + \left(\frac{d\Delta x}{ds}\right)^2}\, ds \approx$$

$$\approx \alpha_0 p + \alpha_1 p^2 + \dots , \tag{2}$$

where L_0 is the length of synchronous orbit, $\rho(s)$ the local radius of curvature, s the longitudinal coordinate. The coefficients α_0 and α_1 are determined as

$$\alpha_0 = \frac{1}{L_0} \oint \frac{D_1}{\rho} ds ; \tag{3a}$$

$$\alpha_1 = \frac{1}{L_0} \oint \left(\frac{D_1'^2}{2} + \frac{D_2}{\rho} \right) ds . \tag{3b}$$

In accordance with the definitions for α_0 and α_1, the momentum compaction factor α_c can be written as

$$\alpha_c = \frac{1}{L_0} \frac{dL}{dp} \approx \alpha_0 + 2\alpha_1 p + \dots . \tag{4}$$

To study the phase dynamics in a storage ring with small momentum compaction factor α_0, the next terms of expansion of the compaction over the energy deviation should be accounted for, hence – higher terms in the sliding factor η [5-7]. Magnitude of η characterizes a relative variation of the phase due to changes of the particle velocity and orbit length. It is determined by the relation

$$\frac{\Delta \phi}{\phi} = \eta(p) p \approx (\eta_0 + \eta_1 p + \dots) p , \tag{5}$$

with η_0 and η_1 having been determined by

$$\eta_0 = \alpha_0 - \frac{1}{\gamma_s^2}, \tag{6a}$$

$$\eta_1 = \alpha_1 + \eta_0 + \frac{3}{2\gamma_s^2}\left(1 - \frac{1}{\gamma_s^2}\right). \tag{6b}$$

The finite-difference equations for the phase ϕ and the variation of relative energy p in the model under consideration read

$$\phi_f = \phi_i + \left(\kappa_0 p_i + \kappa_1 p_i^2\right)\Delta\tau \ ; \tag{7a}$$

$$p_f = p_i - U_{rf}\sin\phi_f \Delta\tau \ , \tag{7b}$$

where

$$\Delta\tau = \tau_f - \tau_i = \frac{\beta c}{L}\left(t_f - t_i\right),$$

the subscripts i and f correspond to the initial and final values, respectively. The dimensionless variable $\tau = t\beta c/L$ represents time expressed in number of rotations (t is time, βc the velocity of a particle). The factors κ_0 and κ_1 at a large γ_s are determined by the expressions $\kappa_0 = 2\pi h\eta_0 \approx 2\pi h\alpha_0$, $\kappa_1 = 2\pi h\eta_1 \approx 2\pi h(\alpha_0+\alpha_1)$ (h is the harmonic number).

From Eqs. (7), differential (smoothed) equations can be deduced. As it seen, the RHS of (7b) contains the final value of the phase ϕ_f expressed via the initial value ϕ_i and momentum p_i by the equation (7a).

Let us expand $\sin\phi_f$ into series of powers of $\Delta\tau$.

$$\sin\phi_f = \sin\left(\phi_i + \left(\kappa_0 p_i + \kappa_1 p_i^2\right)\Delta\tau\right) \approx$$

$$\approx \sin\phi_i + \cos\phi_i\left(\kappa_0 p_i + \kappa_1 p_i^2\right)\Delta\tau \ . \tag{8}$$

Since $\Delta\tau$ cannot be regarded as infinitesimal (formally Eqs. (7) present a full turn, $\Delta\tau = 1$), then the linear term can be neglected if $\kappa_0 p_i + \kappa_1 p_i^2 \ll 1$. In the considered case it can be done since maximum of the energy spread does not exceed a few percents, and the momentum compaction factor α_0 supposed small. From these assumptions, finite difference equations reduce to

$$\frac{\Delta\phi}{\Delta\tau} = \kappa_0 p_i + \kappa_1 p_i^2 ; \tag{9a}$$

$$\frac{\Delta p}{\Delta\tau} = -U_{rf}\sin\phi_i . \tag{9b}$$

3. DIFFERENTIAL MODEL

Noting of formal similarity of Eqs. (8) to the canonical Hamilton equations describing a mathematical pendulum, we can use a smoothed analog to these equations (a differential substitute for a finite-difference equation, $\Delta\tau \to 0$) to facilitate analysis of the motion

$$\frac{d\phi}{d\tau} = \kappa_0 p + \kappa_1 p^2 ; \tag{10a}$$

$$\frac{dp}{d\tau} = -U_{rf}\sin\phi \ . \tag{10b}$$

A Hamilton function associated with (10) possesses a specific form with the cubic canonical momentum term

$$H = \frac{\kappa_1}{3}p^3 + \frac{\kappa_0}{2}p^2 + U_{rf}\left(1 - \cos\phi\right). \tag{11}$$

To analyze a phase portrait of the system, it is convenient to present Hamilton function of the longitudinal motion in the reduced form:

$$\tilde{H} = \mu\frac{\tilde{p}^3}{3} + \frac{\tilde{p}^2}{2} + 1 - \cos\phi \ , \tag{12}$$

where

$$\tilde{p} = \sqrt{\frac{\kappa_0}{U_{rf}}}\,p \approx \sqrt{\frac{2\pi h\alpha_0\gamma_s E_0}{eV_{rf}}}\,p ; \tag{13a}$$

$$\mu^2 = \frac{\kappa_1^2 U_{rf}}{\kappa_0^3} \approx \frac{\left(\alpha_0+\alpha_1\right)^2 eV_{rf}}{2\pi h\alpha_0^3\gamma_s E_0} . \tag{13b}$$

Phase portraits of motion with the Hamiltonian (12) represented in Fig. 1. The magnitude and sign of the parameter μ govern the topology of the phase plane. At zero value, $\mu = 0$, the Hamiltonian (11) or (12) has a form of mathematical pendulum; its phase plane is presented in Fig. 1(a).

Within the interval $0 < \mu^2 < 1/12$, there an additional area of finite motion appears; this area is separated from the main area with the band of infinite motion as depicted in Fig. 1(b). When the parameter μ exceeds the critical value $\mu_c^2 = 1/12$ [see Fig. 1(c)], e.g. $1/12 \le \mu < \infty$, the structure of the phase plane will have changed as is represented in Fig. 1(d).

The dimension of a stable (finite) longitudinal motion, i.e., the area comprised by a separatrix, is in direct proportion with ratio of the ring parameters. For the considered case of the nonlinear Hamiltonian (12), the separatrix height (size along the p axis) is determined by

$$\Delta p = \frac{\alpha_0}{\alpha_0+\alpha_1}\left(\cos\frac{\xi}{3} + \cos\left(\frac{\xi}{3} + \frac{\pi}{3}\right)\right), \tag{14a}$$

$$\cos\xi = 12U_{rf}\frac{\left(\alpha_0+\alpha_1\right)^2}{\pi h\alpha_0^3} - 1 ,$$

$$\Delta p = \frac{3}{2}\frac{\alpha_0}{\alpha_0+\alpha_1} , \tag{14b}$$

for $\mu \le \mu_c$ (14a) and $\mu \ge \mu_c$ (14b), respectively.

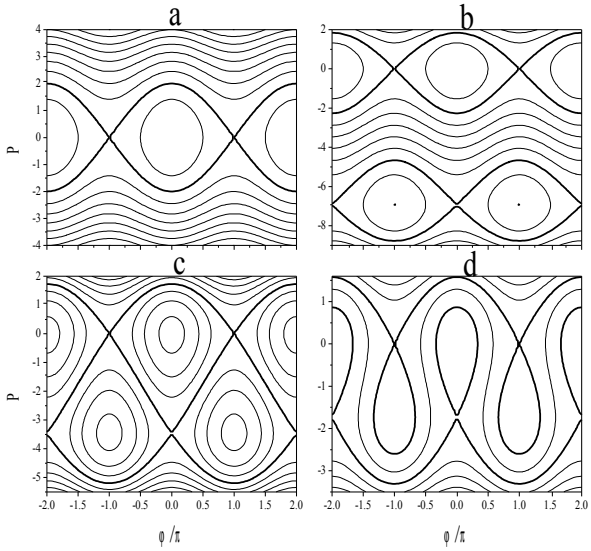

Fig. 1. *Phase portrait of longitudinal motion with account for the cubic nonlinearity at different values of the parameter μ. (a): $\mu = 0$, (b): $\mu \le |\mu_c|$, (c): $\mu = \mu_c$, $\mu \ge |\mu_c|$*

The phase width of the separatrix (dimension along the ϕ axis) is determined by expressions

$$\Delta\phi = 2\pi \; ; \qquad \mu \le \mu_c , \qquad (15a)$$

$$\Delta\phi = 2\arccos\left(1 - \frac{\pi h}{3U_{rf}}\frac{\alpha_0^3}{(\alpha_0+\alpha_1)^2}\right); \; \mu \ge \mu_c \qquad (15b)$$

for the sub- and overcritical values of the parameter μ.

Dependence of the phase and momentum separatrix extensions on rf amplitude at fixed other parameters, which values are listed in the table, is presented in Fig. 2.

Ring parameters

parameter	desig	value
Accel. voltage (Volt)	V_{rf}	$4\text{x}10^5$
Lorentz factor	γ	84
Harmonic number	h	32
Linear comp. factor	α_0	0.01
Quad. comp. factor	α_1	0.2

As it can be seen from the plot in Fig. 2, while increasing the parameter U_{rf}, the separatrix height grows up reaching its maximum, $\Delta p \approx 7.1\times10^{-2}$, at $U_{rf} \approx 3.8\times10^{-4}$ (which is equal to the rf voltage of $V_{rf} \approx 16.3$ kV at γ_s=84).

With further increase in the rf voltage, the separatrix height remains constant. The separatrix width remains constant with increase of the rf voltage up to the critical value U_{rf}, then it is diminishing.

In Fig. 3, a dependence of the separatrix dimensions upon the linear momentum compaction factor under other system parameters fixed is presented.

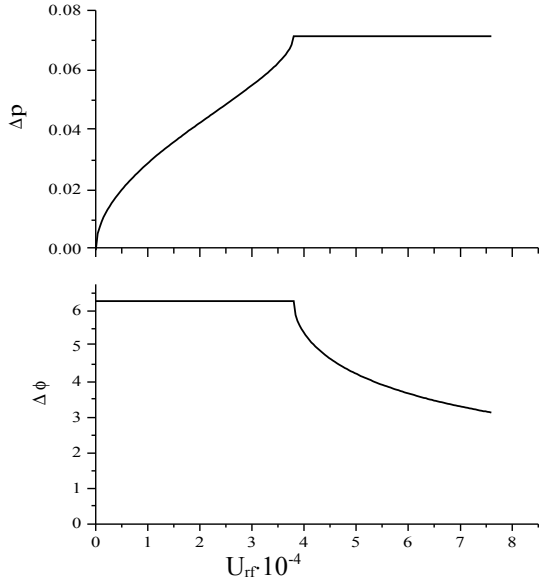

Fig. 2. *Separatrix height (top) and width (bot) vs U_{rf}*

Quite the reverse to the dependence $\Delta\phi = \Delta\phi(U_{rf})$, a dependence of the separatrix width upon the linear compaction factor, $\Delta\phi = \Delta\phi(\alpha_0)$, is increasing while α_0 grows. At a certain critical value of the linear momentum compaction factor $\alpha_{0(c)}$ (in the suggested case $\alpha_{0(c)} \approx 0.03$), the width of equilibrium area has reached its maximum and remains constant with further increase in α_0. A dependence of the separatrix height on α_0 is of increasing within interval $0 \le \alpha_0 \le \alpha_{0(c)}$. Then, after the maximum at $\alpha_0 = \alpha_{0(c)}$ this dependence becomes declining, coming to zero at a large α_0.

Since the phase volume enclosed within the separatrix (and, therefore, the storage ring acceptance) is proportional to product of the transverse dimensions of the separatrix, $\sigma \sim \Delta p \Delta\phi$, then from comparison of the plots in Fig. 2 and Fig. 3 it follows that optimal working point is about the critical parameters.

In addition, it can be seen that, dislike a linear lattice, nonlinear terms in the momentum compaction factor restrict the infinite increase of energy acceptance with decreasing of the linear momentum compaction factor: The acceptance increase takes place while the linear compaction is above certain critical value $\alpha_{0(c)}$, which is determined by the ring lattice parameters according to equality

$$\frac{(\alpha_0+\alpha_1)^2 eV_{rf}}{2\pi h \alpha_0^3 \gamma_s E_0} = \frac{1}{12} . \qquad (16)$$

With further decrease of α_0 the acceptance also decreases.

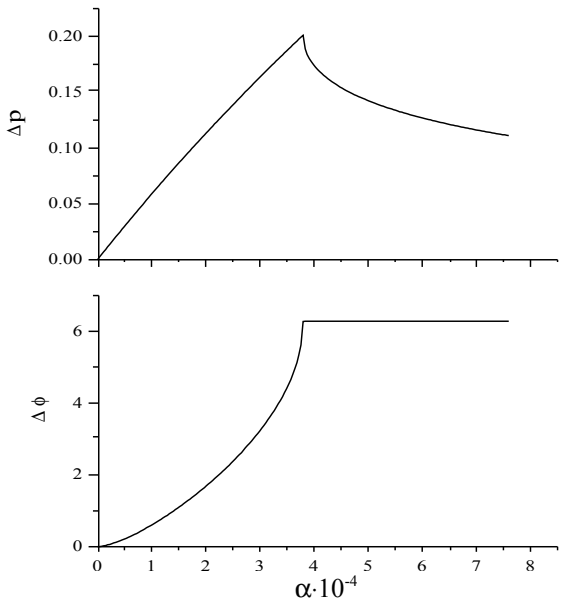

Fig. 3. *Separatrix height (top) and width (bottom) vs α_0*

To validate the use of differential (smoothed) equations of motion (10) for analysis of Compton storage ring, a code has been developed based on the finite difference equations (7). A simulated phase space portrait at the ring parameters listed in the table for $\mu \ge \mu_c$ is presented in Fig. 4.

From the figure it follows that the electrons can be confined within not only the "linear" area (minimum of Hamilton function (12)), but "nonlinear" as well. (The nonlinear stable region disappears in a linear lattice.) RMS sizes and the center of weight positions perfectly correspond to the analytical estimations presented above.

4. SUMMARY. CONCLUSION

Results of the study on dynamics of synchrotron motion of particles in the storage rings with the nonlinear momentum compaction factor presented in the paper, can be digested as follows:

Grounded on a simplified model of the storage ring, the finite-difference equations were derived. Hamiltonian treatment of the phase space structure was performed. As was shown, the structure of the phase space is governed by ratios of the ring parameters. An analytical expression for the factor μ, which determines the topology of the longitudinal phase space, was derived.

Dependencies of the sizes of the equilibrium areas of the synchrotron motion in a nonlinear lattice were derived. Analysis of dependence of the longitudinal acceptance upon the amplitude of rf voltage, and the linear compaction factor at the fixed quadratic nonlinear term was presented.

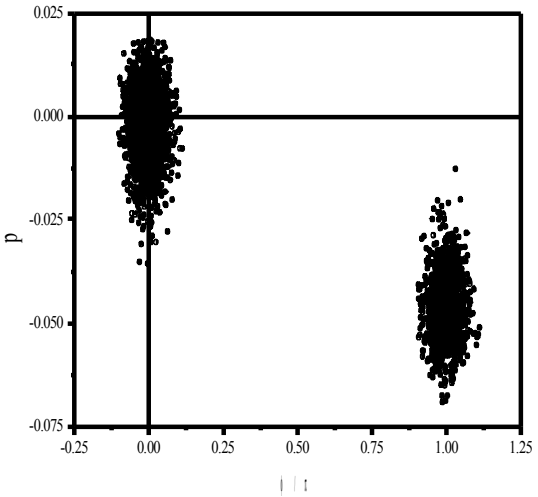

Fig. 4. *Distribution of confined electrons over the longitudinal phase plane in a system with cubic nonlinearity at $\mu \geq \mu_c$; left bunch corresponds to "linear" case, right - to "nonlinear" (additional)*

As was shown, the acceptance is growing up only to a definite magnitude, which determines by the critical value of parameter $\mu = \mu_c$. It was emphasized that in order to maximize the acceptance of a lattice with a small linear momentum compaction factor and a wide energy spread of electrons in the bunches, the system parameters should be chosen close to the critical value of μ.

To validate the use of smoothed equations of motion, a simulating code was developed. The code is based on the finite-difference equations. The results of simulation manifest a good agreement with the theoretical predictions on the sizes and position of equilibrium areas.

The results obtained allow to make the following conclusion: Enlargement of the energy acceptance of a ring by decreasing of the momentum compaction factor is limited with the nonlinearity in the compaction factor. Decreasing of the linear compaction factor below the certain limit causes the reversed effect – decreasing of the acceptance.

Similar consequence corresponds to the build-up of the rf voltage: Increase of the voltage above a certain limit causes narrowing of possible bunch length while the energy acceptance remains constant. This effect can lead to decrease in the injection efficiency for high rf voltages.

REFERENCES

1. Z. Huang, R.D. Ruth. Laser-electron storage ring // *Phys. Rev. Lett.* 1998, v. 80, p. 976-979.
2. R.J. Loewen. *A compact light source: design and technical feasibility study.* Ph.D. thesis, Stanford 2003.
3. P.I. Gladkikh. Lattice and beam parameters of compact intense X-ray source based on Compton scattering // *Phys. Rev. ST Accel Beams.* 2005, v. 8, 050702.
4. E.V. Bulyak. *Laser cooling of electron bunches in Compton storage rings*. Proc. EPAC-2004 http://accelconf.web.CERN.ch/accelconf/e04/papers/.
5. C. Pellegrini, D. Robin. Quasiisochronous storage ring *// NIM.* 1991, v. A301, p. 27-36.
6. Liu Lin, E.T. Gonsalves da Silva. // Second order single particle dynamics in quasiisochronous storage rings and its applications to the LNLS-UVX ring *// NIM.* 1993, v. A329, p. 9-15.
7. J. Feikes et al. The BESSY low alpha optics and the generation of coherent synchrotron radiation // *ICFA Beam dynamics newsletter.* 2004, v. 35, p. 82-95.

ИССЛЕДОВАНИЕ СИНХРОТРОННОГО ДВИЖЕНИЯ В КОМПТОНОВСКОМ ИСТОЧНИКЕ

Е.В. Буляк, П.И. Гладких, В.В. Скоморохов

Исследована продольная динамика электронных сгустков в накопителях с малым коэффициентом упаковки орбит и с большим энергетическим разбросом электронов в пучке. Рассмотрена структура фазового пространства и его деформация при изменении параметров накопительного кольца. Показана зависимость размеров области устойчивости продольного движения от параметров накопителя при нелинейной структуре уравнений движения.

ДОСЛІДЖЕННЯ СИНХРОТРОННОГО РУХУ У КОМПТОНІВСЬКОМУ ДЖЕРЕЛІ

Є.В. Буляк, П.І. Гладких, В.В. Скоморохов

Досліджено подовжню динаміку електронних згустків у нагромаджувачі з малим коефіцієнтом упаковки орбіт та великим енергетичним розкидом електронів у пучку. Розглянуто структуру фазового простору та його деформацію при зміні параметрів нагромаджувального кільця. Показано залежність розмірів області стійкості подовжнього руху від параметрів нагромаджувача при нелінійній структурі рівнянь руху.